
This is an electronic reprint of the original article.
This reprint may differ from the original in pagination and typographic detail.

Shen, Fuhui; Pan, Boyu; Wang, Shufan; Lian, Junhe; Münstermann, Sebastian
Influence of Stress States on Cleavage Fracture in X70 Pipeline Steels

Published in:
Journal of Pipeline Science and Engineering

DOI:
[10.1016/j.jpse.2022.100072](https://doi.org/10.1016/j.jpse.2022.100072)

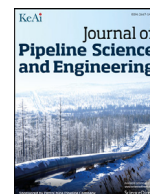
Published: 01/09/2022

Document Version
Publisher's PDF, also known as Version of record

Published under the following license:
CC BY-NC-ND

Please cite the original version:
Shen, F., Pan, B., Wang, S., Lian, J., & Münstermann, S. (2022). Influence of Stress States on Cleavage Fracture in X70 Pipeline Steels. *Journal of Pipeline Science and Engineering*, 2(3), [100072].
<https://doi.org/10.1016/j.jpse.2022.100072>

This material is protected by copyright and other intellectual property rights, and duplication or sale of all or part of any of the repository collections is not permitted, except that material may be duplicated by you for your research use or educational purposes in electronic or print form. You must obtain permission for any other use. Electronic or print copies may not be offered, whether for sale or otherwise to anyone who is not an authorised user.



Influence of stress states on cleavage fracture in X70 pipeline steels

Fuhui Shen^{a,*}, Boyu Pan^a, Shufan Wang^a, Junhe Lian^b, Sebastian Münstermann^a

^a Integrity of Materials and Structures, Steel Institute, RWTH Aachen University, Intzestraße 1, Aachen 52072, Germany

^b Advanced Manufacturing and Materials, Department of Mechanical Engineering, Aalto University, Puumiehenkuja 3, Espoo 02150, Finland

ARTICLE INFO

Keywords:

Stress triaxiality
 Cleavage fracture
 Plasticity
 Anisotropy

ABSTRACT

Stress state is a primary factor controlling the ductile fracture behavior of steels, which is typically represented as the combination of the stress triaxiality and Lode angle parameter. The cleavage fracture properties of pipeline steels at low temperatures are usually assessed under plane strain conditions, such as using the fracture mechanics experiments. In this study, the cleavage fracture properties of a X70 steel at liquid nitrogen temperature ($-196\text{ }^{\circ}\text{C}$) are characterized over a broad range of stress states. A comprehensive experimental program is carried out by performing tensile tests using various flat specimens of different geometries immersed in liquid nitrogen, including shear, central hole, notched dog bone, and side grooved plane strain. Pronounced plasticity occurs prior to the final fracture within the tested range of stress states at the very low temperature. Anisotropy effects are considered by conducting tensile tests of fracture specimens along the rolling, diagonal and transverse directions. Finite element simulations of corresponding experiments are performed using an evolving quadratic plasticity model to extract the local stress state variables to establish the fracture criteria, which are formulated based on the critical values of plastic strain and maximum principal stress. The fracture strain of the investigated material at liquid nitrogen temperature is affected by the stress triaxiality, Lode angle parameter and loading direction.

1. Introduction

The prediction and prevention of cleavage fracture are of critical importance for the integrity of pipeline structures. Fracture mechanics tests with pre-crack configurations at low temperatures are widely used to evaluate the cleavage fracture properties of steels with a body-centered cubic structure. The plane strain condition and high stress triaxiality in the fracture mechanics specimens are adopted to obtain conservative fracture toughness results (Anderson, 2017). It is also essential to understand and predict the cleavage fracture behavior under other loading conditions, with low to medium stress triaxiality, which has not been fully explored.

The effects of stress states on ductile fracture have been investigated in many damage mechanics studies, where a category of specimen geometries is used to achieve a broad range of stress states (Lian et al., 2012; Li et al., 2011; Mu et al., 2020; Dunand and Mohr, 2010). The recent development of ductile fracture models has revealed the effects of the third stress invariant on ductile fracture behavior (Bai and Wierzbicki, 2008; Shen et al., 2022; Xue, 2007, 2008; Rice and Tracey, 1969; Bai and Wierzbicki, 2009; Lou et al., 2014; Mohr and Marcadet, 2015). The triaxiality dependence of cleavage fracture has been reported in some studies (Bass et al., 1999; Testa et al., 2020). However, the influence of stress states on cleavage fracture, considering both stress triaxiality and Lode angle parameter, has only re-

ceived relatively limited research attention. Even though the commercial pipeline structures are not likely to be used at temperatures below their ductile to brittle transition temperatures, a comprehensive characterization of the fracture behavior of a pipeline steel over a broad range of stress states is of critical importance.

To achieve an accurate prediction of fracture with the failure criteria, the local stress and strain fields under different mechanical loading conditions need to be precisely described by numerical models (Beremin, 1983; Pineau et al., 2016; Pineau and Tanguy, 2010). Due to the manufacturing history of pipeline steels, a certain degree of anisotropy is usually observed in the mechanical properties, which can be described using various constitutive models (Shinohara et al., 2016). When significant plastic deformation occurs prior to final fracture in modern steels with high toughness, the accuracy of the applied constitutive model is playing a more critical role in the prediction of final fracture. Therefore, it is aimed to perform an experimental and numerical study to characterize the cleavage fracture of a pipeline steel considering the effects of stress states and anisotropy in this study.

2. Material and experiments

To characterize the effects of stress state on the cleavage fracture of a X70 pipeline steel, tensile tests have been performed using five different specimen geometries, which are immersed in liquid nitrogen.

* Corresponding author.

E-mail address: fuhui.shen@iehk.rwth-aachen.de (F. Shen).

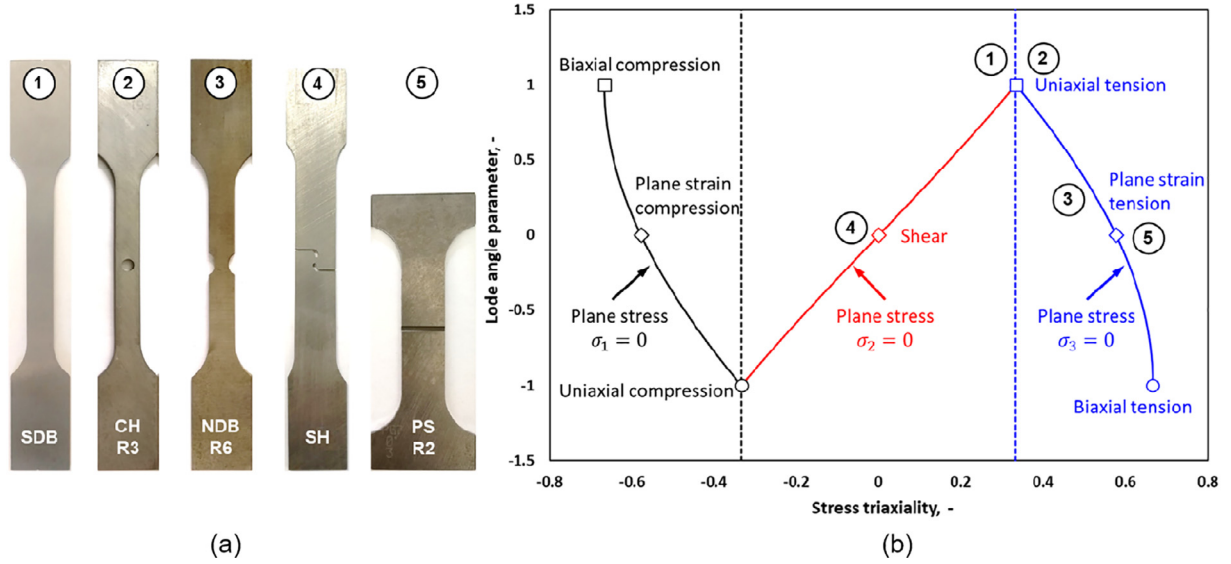


Fig. 1. Demonstration of (a) specimen geometry and (b) corresponding stress states, modified from Bai and Wierzbicki (2008).

Flat tensile specimens with a thickness of 2 mm have been manufactured out of a strip. The smooth dog bone (SDB) specimen is used to characterize the uniaxial tensile properties of the material. The central hole (CH), notched dog bone (NDB), shear (SH) and plane strain (PS) specimens are used to investigate the fracture behavior under different stress states. The sample geometries and corresponding stress states are demonstrated in Fig. 1. To consider the effects of anisotropy, all tensile specimens have been manufactured along three directions (00°, 45° and 90°) with respect to the rolling direction, which is perpendicular to the longitudinal direction of the pipeline. In this study, only tension-dominated stress states (with zero and positive stress triaxiality) are considered in the experimental program.

Tensile tests have been performed using a Zwick machine under quasi-static conditions with a crosshead speed of 0.4 mm/min. A container filled with liquid nitrogen is attached to the tensile machine, as shown in Fig. 2. Before starting the tests, the specimens have been immersed entirely in liquid nitrogen and held for several minutes to reach the desired temperature. During the tests, the force has been recorded by the load cell. The recorded crosshead displacement has been converted into the final displacement corresponding to a gauge length of 40 mm based on the experimental results at room temperature with the identical geometry (Shen et al., 2020).



Fig. 2. Experimental setup for tensile tests at liquid nitrogen temperature.

3. Models

The pronounced plastic deformation behavior prior to final fracture is described by an evolving quadratic plasticity model, which has been proposed by Lian et al. (2018) and applied to describe the anisotropic deformation of different materials (Shen et al., 2021). The anisotropic effects in plasticity are captured by the Hill48 equivalent stress in the yield criterion described in Eq. (1). The temperature effects on the anisotropic plasticity behavior of this material can be described by a thermal-dependent constitutive model developed by Shen et al. (2020), where the flow stress is formulated as functions of plastic strain, temperature and loading orientation. To achieve a more accurate description of the plastic deformation, the anisotropic parameters in Eq. (2) have been calibrated as continuous functions of plastic strain based on flow curves obtained from uniaxial tensile tests at -196 °C.

$$f = \bar{\sigma}(\sigma, F, G, H, L, M, N) - \sigma_Y(\bar{\epsilon}^p) \leq 0 \quad (1)$$

$$\bar{\sigma}(\sigma) = \left\{ \frac{1}{2} \left[F(\sigma_{22} - \sigma_{33})^2 + G(\sigma_{33} - \sigma_{11})^2 + H(\sigma_{11} - \sigma_{22})^2 \right] + L\sigma_{23}^2 + M\sigma_{13}^2 + N\sigma_{12}^2 \right\}^{\frac{1}{2}} \quad (2)$$

The stress states can be explicitly described by the combination of stress triaxiality and Lode angle parameter, and some characteristic stress states are summarized in Fig. 1. The stress triaxiality η and Lode angle parameter $\bar{\theta}$ are derived from the Cauchy (σ) and deviatoric (s) stress invariants, according to Bai and Wierzbicki (2008).

$$I_1 = \text{tr}(\sigma) \quad (3)$$

$$J_2 = \frac{1}{2} \text{tr}(s^2) \quad (4)$$

$$J_3 = \det(s) = \frac{1}{3} \text{tr}(s^3) \quad (5)$$

$$\eta = I_1 / \sqrt{27J_2} \quad (6)$$

$$\bar{\theta} = 1 - \frac{6}{\pi} \theta = 1 - \frac{2}{\pi} \cos^{-1} \left(\sqrt{27/4} J_3 J_2^{-3/2} \right) \quad (7)$$

As the cleavage fracture process is typically composed of microcrack initiation and crack propagation steps, a generalized Orowan fracture model has been proposed by He et al. (2017). In this fracture model, a stress state dependent critical plastic strain is adopted as the criterion for microcrack initiation, while a critical value of the maximum principal stress is defined as the crack propagation criterion ($\sigma_1 \geq \sigma_c$). The stress state dependence of the microcrack initiation strain is described by a phenomenological function in Eq. (8). The probabilistic features of cleavage fracture are also considered in the cleavage fracture model in Eq. (9), where the failure probability is described using a Weibull distribution function. A more detailed description of the fracture criterion can be found in Shen et al. (2022).

$$\bar{\varepsilon}_{mci}(\eta, \bar{\theta}) = (C_1 \exp^{-C_2 \eta} - C_3 \exp^{-C_4 \eta}) \bar{\theta}^2 + C_3 \exp^{-C_4 \eta} \quad (8)$$

$$P_f = 1 - \exp \left[- \left(\frac{\bar{\varepsilon}_{mci} - \bar{\varepsilon}_{\min}}{\bar{\varepsilon}_u - \bar{\varepsilon}_{\min}} \right)^m \right] \quad (9)$$

4. Results

To consider the probabilistic characteristics of cleavage fracture behavior, seven repeating tests have been conducted for each loading condition. The results from individual tests and the average results of the force and displacement curves as well as the fracture points are shown in Fig. 3 for the notched dog bone (NDB-R6) specimen along the 45°. The overall very good repeatability is observed in the experimental results. Therefore, the average results of the force and displacement curves in combination with a scatter band are used in the following to represent the experimental results for each loading configuration. From the experimental results of the NDB-R6 geometry shown in Fig. 3, it is evident that a significant amount of plastic deformation occurs prior to fracture in the material at liquid nitrogen temperature. In addition, both the force and the final fracture displacement are dependent on the loading direction, while the scatter in the fracture displacements is not very pronounced. The fracture surface of the NDB-R6 sample along the 45° is shown in Fig. 4, which is mainly composed of cleavage facets in these specimens. These experimental results provide evidence that cleavage fracture in bcc steels can be triggered after significant plastic deformation at such low temperatures, depending on the microstructure and loading conditions.

The finite element models of tensile specimens have been created with a fine mesh ($0.1 \times 0.1 \times 0.1 \text{ mm}^3$) in the critical deformation

region. The anisotropic hardening is described by calibrating the individual flow curves along three loading directions based on uniaxial tensile tests at $-196 \text{ }^\circ\text{C}$. The calibration and validation procedures of model parameters are similar to those described in ductile fracture simulations (Shen et al., 2020). The force and displacement curves of the tensile tests using the NDB-R6 geometry along three loading directions (00° , 45° and 90°) are shown in Fig. 5. The simulation results with the evolving plasticity model are shown as solid curves, which are in good agreement with the average experimental results represented by dotted curves.

The local stress states of the critical elements in tensile specimens are extracted from finite element simulation results. The critical element is located at the symmetrical center in the notched dog bone specimens. The accumulation of the equivalent plastic strain (PEEQ) and the evolution of local stress state variables, stress triaxiality and Lode angle parameter, in the NDB-R6 geometry are shown in Fig. 6 for three loading directions. The open symbols are corresponding to the average fracture points for three directions. It is evident that both the equivalent plastic strain at fracture and the history of local stress states are affected by the loading direction, which is due to anisotropic effects. To consider the effects of loading history, the averaged stress triaxiality and Lode angle parameter are used to represent the overall local stress states.

Based on the seven parallel tests for each geometry and loading direction, the distribution of the equivalent plastic strain at fracture obtained from individual tests is described by a Weibull distribution function, which is shown in Fig. 7. Solid symbols are corresponding to seven repeating experimental results. Solid curves are corresponding to the fitting results of Weibull distribution functions with optimized parameters ($\bar{\varepsilon}_u$, $\bar{\varepsilon}_{\min}$ and m) according to Eq. (9). In addition, the local maximum principal stress at fracture is also collected for different geometries. With the collected local stress state variables and critical values of plastic strain and stress, the stress state dependent fracture criterion at liquid nitrogen temperature can be established for the material under the investigated loading conditions. The calibrated fracture locus along the 45° direction corresponding to three different failure probabilities is also shown in Fig. 7 under the plane stress condition. Given the results along the 45° direction as an example, it is noticed that the fracture strain shows non-monotonic dependence on the stress triaxiality. The fracture strain under shear conditions is lower than that under uniaxial tension conditions, which is due to the fact that the Lode angle also affects the fracture strain.

Understanding the cleavage fracture is of crucial importance for the integrity of pipeline structures. At extremely low temperatures, cleavage

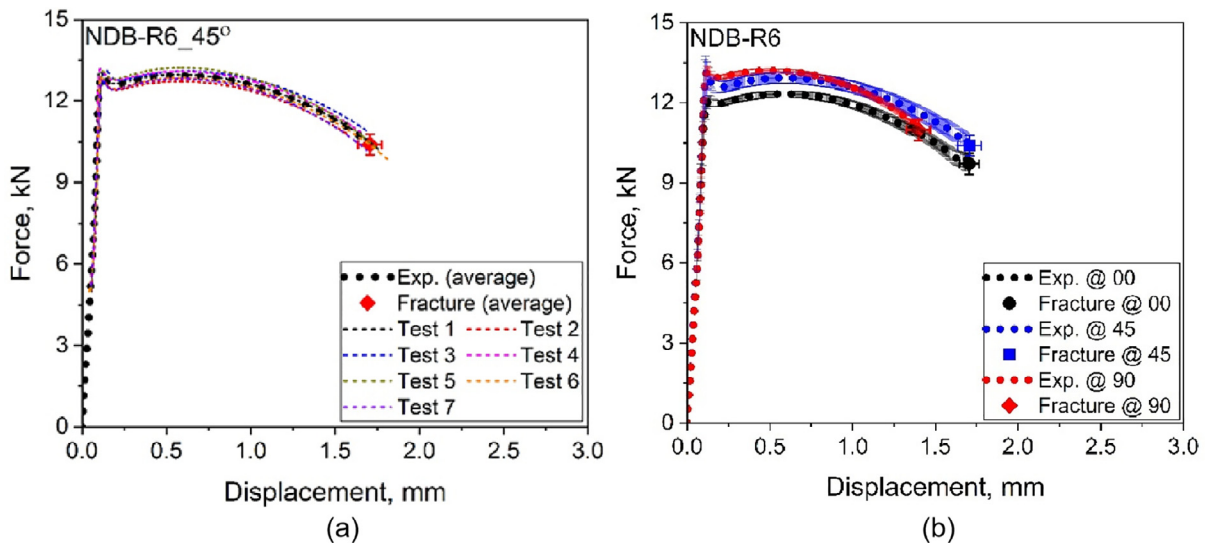


Fig. 3. Experimental results of tensile tests using notched dog bone specimen at liquid nitrogen temperature.

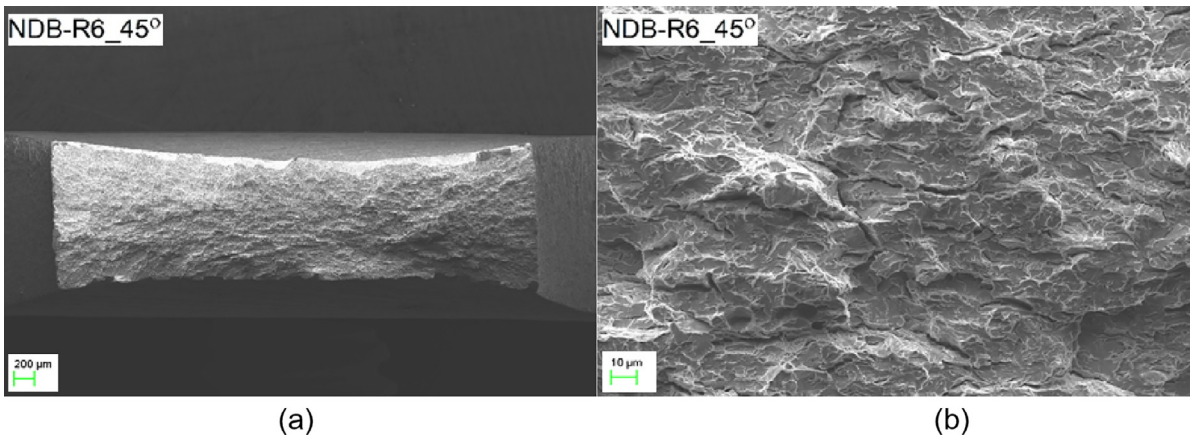


Fig. 4. Fracture surface of notched dog bone specimens after tensile tests at liquid nitrogen temperature.

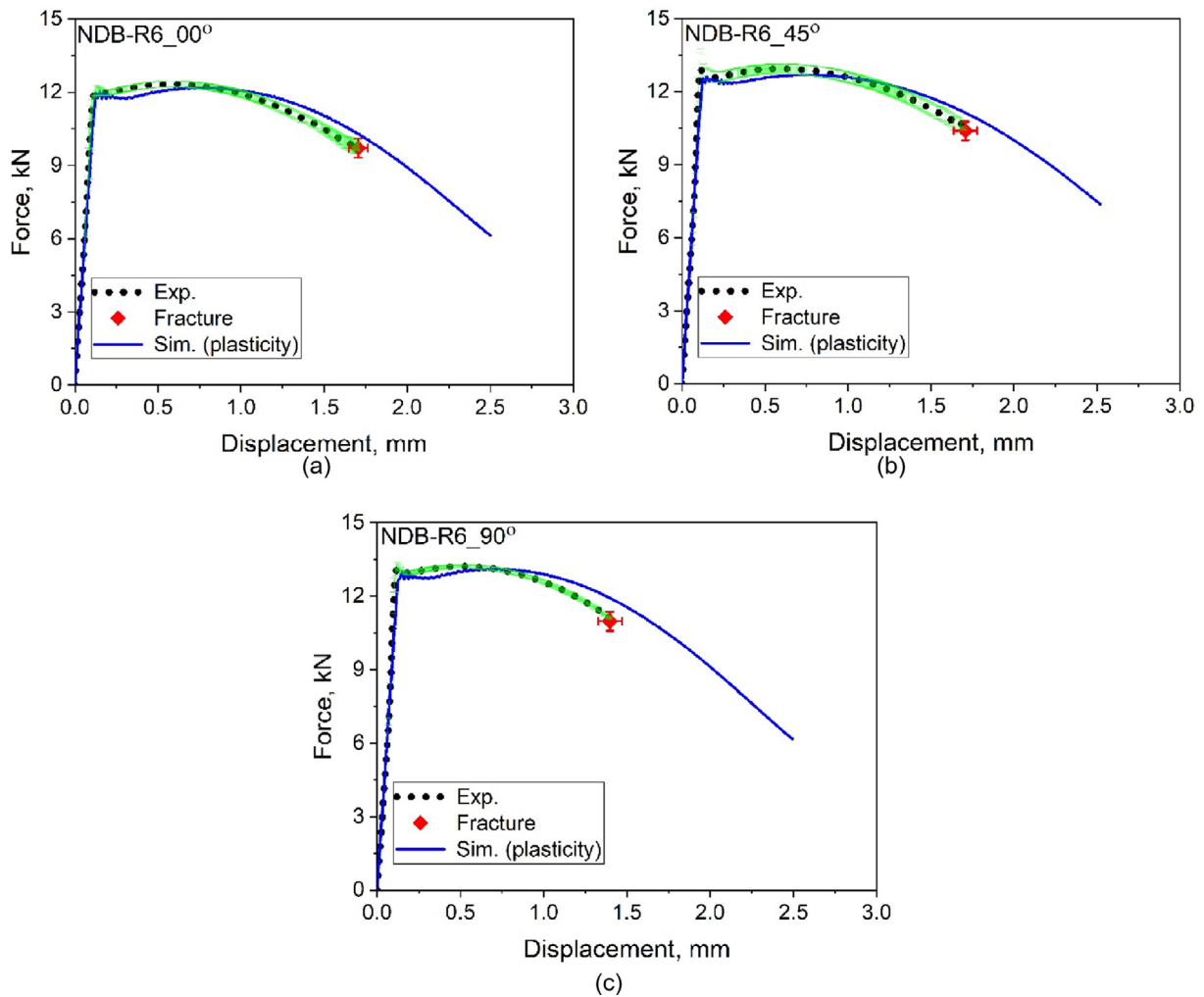


Fig. 5. Force and displacement curves of tensile tests using notched dog bone specimens at $-196\text{ }^{\circ}\text{C}$.

fracture is expected to occur without macroscopic plasticity in typical pipeline steels. To avoid catastrophic failure, the well-established strategy is to select materials that provide sufficient toughness properties under application conditions. The results obtained in this study provide essential evidence that cleavage fracture can be triggered after significant plastic deformation at temperatures far below the ductile to brittle

transition temperature under controlled loading conditions. Therefore, an important insight obtained from this study is that stress state, in addition to temperature, plays significant roles in determining the fracture behavior of the pipeline steels as well. Controlling the loading condition, e.g., stress state, is also a promising strategy to improve the safety of steel infrastructures under operating conditions.

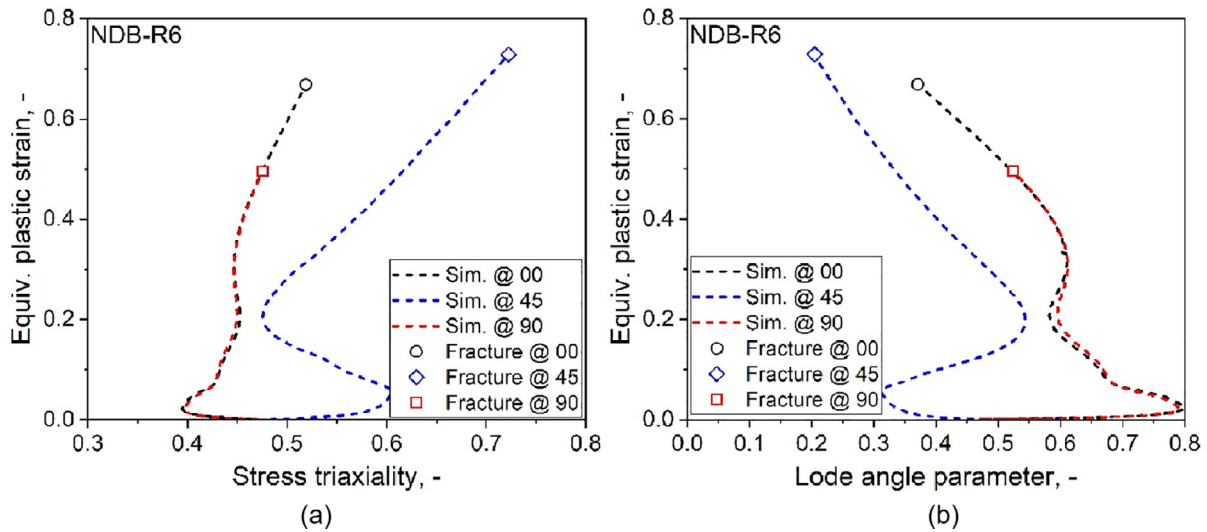


Fig. 6. Evolution of local stress states during tensile tests using notched dog bone specimens at $-196\text{ }^{\circ}\text{C}$.

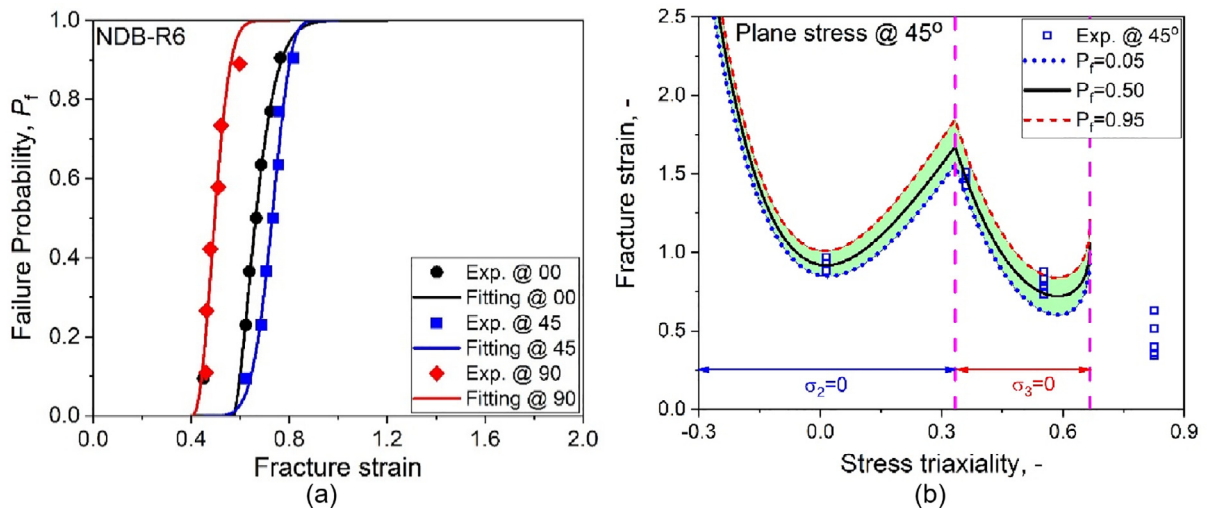


Fig. 7. Probabilistic distribution of fracture strain in the notched dog bone specimens and the fracture locus along the 45° at liquid nitrogen temperature.

5. Conclusions

Tensile tests have been performed at liquid nitrogen temperature using different flat specimen geometries to characterize the effects of stress states on cleavage fracture in this study. Some important conclusions are summarized as follows:

- (1) Pronounced plastic deformation occurs prior to cleavage fracture in the flat tensile specimens of the X70 pipeline steel at liquid nitrogen temperature.
- (2) The cleavage fracture of the X70 steel also shows dependence on stress states, which can be considered by the stress state dependent microcrack initiation strain criterion under the investigated loading conditions.
- (3) Both the plastic deformation and cleavage fracture properties are affected by the loading direction. An anisotropic constitutive model is applied to describe the deformation behavior at liquid nitrogen temperature.

Declaration of Competing Interest

The authors declare that they have no known competing financial interests or personal relationships that could have appeared to influence the work reported in this paper.

Acknowledgments

thyssenkrupp Steel Europe AG is gratefully acknowledged for materials supply and financial support. Simulations were performed with computing resources granted by RWTH Aachen University under project rwth0241.

References

Anderson, T.L., 2017. Fracture mechanics: fundamentals and applications. CRC press.
 Lian, J., Sharaf, M., Archie, F., Münstermann, S., 2012. A hybrid approach for modelling of plasticity and failure behaviour of advanced high-strength steel sheets. *Int. J. Damage Mech.* 22 (2), 188–218.

- Li, H., Fu, M.W., Lu, J., Yang, H., 2011. Ductile fracture: Experiments and computations. *Int. J. Plast.* 27 (2), 147–180.
- Mu, L., Jia, Z., Ma, Z., Shen, F., Sun, Y., Zang, Y., 2020. A theoretical prediction framework for the construction of a fracture forming limit curve accounting for fracture pattern transition. *Int. J. Plast.* 129.
- Dunand, M., Mohr, D., 2010. Hybrid experimental–numerical analysis of basic ductile fracture experiments for sheet metals. *Int. J. Solids Struct.* 47 (9), 1130–1143.
- Bai, Y., Wierzbicki, T., 2008. A new model of metal plasticity and fracture with pressure and Lode dependence. *Int. J. Plast.* 24 (6), 1071–1096.
- Shen, F., Wang, H., Liu, Z., Liu, W., Könemann, M., Yuan, G., et al., 2022. Local formability of medium-Mn steel. *J. Mater. Process. Technol.* 299.
- Xue, L., 2007. Damage accumulation and fracture initiation in uncracked ductile solids subject to triaxial loading. *Int. J. Solids Struct.* 44 (16), 5163–5181.
- Xue, L., 2008. Constitutive modeling of void shearing effect in ductile fracture of porous materials. *Eng. Fract. Mech.* 75 (11), 3343–3366.
- Rice, J.R., Tracey, D.M., 1969. On the ductile enlargement of voids in triaxial stress fields. *J. Mech. Phys. Solids* 17 (3), 201–217.
- Bai, Y., Wierzbicki, T., 2009. Application of extended Mohr–Coulomb criterion to ductile fracture. *Int. J. Fract.* 161 (1), 1–20.
- Lou, Y., Yoon, J.W., Huh, H., 2014. Modeling of shear ductile fracture considering a changeable cut-off value for stress triaxiality. *Int. J. Plast.* 54, 56–80.
- Mohr, D., Marcadet, S.J., 2015. Micromechanically-motivated phenomenological Hosford–Coulomb model for predicting ductile fracture initiation at low stress triaxialities. *Int. J. Solids Struct.* 67–68, 40–55.
- Bass, B.R., McAfee, W.J., Williams, P.T., Pennell, W.E., 1999. Fracture assessment of shallow-flaw cruciform beams tested under uniaxial and biaxial loading conditions. *Nucl. Eng. Des.* 188 (3), 259–288.
- Testa, G., Bonora, N., Ruggiero, A., Iannitti, G., Gentile, D., 2020. Stress triaxiality effect on cleavage fracture stress. *Theor. Appl. Fract. Mech.* 109, 102689.
- Beremin, F.M., 1983. A local criterion for cleavage fracture of a nuclear pressure vessel steel. *Metall. Trans. A* 14 (11), 2277–2287.
- Pineau, A., Benzerga, A.A., Pardoën, T., 2016. Failure of metals I: Brittle and ductile fracture. *Acta Mater.* 107, 424–483.
- Pineau, A., Tanguy, B., 2010. Advances in cleavage fracture modelling in steels: Micromechanical, numerical and multiscale aspects. *Comptes Rendus Phys.* 11 (3–4), 316–325.
- Shinohara, Y., Madi, Y., Besson, J., 2016. Anisotropic ductile failure of a high-strength line pipe steel. *Int. J. Fract.* 197 (2), 127–145.
- Shen, F., Münstermann, S., Lian, J., 2020. Investigation on the ductile fracture of high-strength pipeline steels using a partial anisotropic damage mechanics model. *Eng. Fract. Mech.* 227, 106900.
- Lian, J., Shen, F., Jia, X., Ahn, D.-C., Chae, D.-C., Münstermann, S., et al., 2018. An evolving non-associated Hill48 plasticity model accounting for anisotropic hardening and r -value evolution and its application to forming limit prediction. *Int. J. Solids Struct.* 151, 20–44.
- Shen, F., Münstermann, S., Lian, J., 2021. Forming limit prediction by the Marciniak–Kuczynski model coupled with the evolving non-associated Hill48 plasticity model. *J. Mater. Process. Technol.* 287, 116384.
- Shen, F., Münstermann, S., Lian, J., 2020. An evolving plasticity model considering anisotropy, thermal softening and dynamic strain aging. *Int. J. Plast.* 132, 102747.
- He, J., Lian, J., Golisch, G., Jie, X., Münstermann, S., 2017. A generalized Orowan model for cleavage fracture. *Eng. Fract. Mech.* 186, 105–118.
- Shen, F., Münstermann, S., Lian, J., 2022. A unified fracture criterion considering stress state dependent transition of failure mechanisms in bcc steels at $-196\text{ }^{\circ}\text{C}$. *Int. J. Plast.* Accepted.